

# Mathematical Modeling of an electro-hydraulic actuator for humanoid robots

A. ABDELLATIF<sup>1</sup>, SAMER ALFAYAD\*<sup>1</sup>, FETHI B. OUEZDOU<sup>1</sup>, SALEM A. HAGGAG<sup>2</sup>, FAYCAL NAMOUN<sup>3</sup>

<sup>1</sup>Laboratoire d'Ingénierie des Systèmes de Versailles (LISV), EA4048 Université de Versailles Saint-Quentin-en-Yvelines, Paris-Saclay University, Vélizy, France.

<sup>2</sup>School of Engineering, Department of Mechanical Engineering, P. O. Box 28282, Dubai, United Arab Emirates.

<sup>3</sup>BIA ZA Les Boutriers, 8 rue de l'Hautil, 78000 Conflans fin d'Oise, FRANCE.

\*samer.alfayad@lisv.uvsq.fr

*Abstract:* - The work presented in this paper is based on a novel integrated and compact hydraulic robotic actuator [1] (BIA patent- US20110085922), intended for the hydraulic humanoid robot HYDROiD. This actuator solves the problem of autonomy for hydraulic humanoid robots as it can be integrated to operate each joint separately. Thus, eliminating the need for a central hydraulic power pack. Also, due to its small size, it can be placed as near as possible to the robot joints to minimize the possible drawbacks of hydraulic actuation units. The main problem for this prototype came from its compactness, causing the inability to study the dynamic properties of this hydraulic actuator such as leakage, friction and compressibility. Therefore, any enhancement or modification for its tiny mechanical components for performance improvement is not possible. As it lacks a mathematical model that represent the dynamics of the system at hand. Here comes the contribution of this paper, where a detailed mathematical model for the actuator is presented and simulated using MATLAB/Simulink. To validate this model, a sim-mechanics model based on its actual CAD design was presented and the two models were compared to verify the deduced dynamic model for the system. The results showed the accuracy of proposed mathematical model as a vital tool to represent the actuator and enhance it in future prototypes.

*Key-Words:* - Hydraulic Actuation, Integration Technology, Humanoid robot, HYDROiD Robot, Dynamic model, System verification.

## 1 Introduction

The development of bio-inspired robots has been going on for the past few years. These robots combine many desirable features such as human-like locomotion capabilities and human-friendly design and behavior [2]. However, the performances exhibited by bio-inspired robots depends mainly on its actuation. Research in the actuation of bio-inspired robots has been investigated by several research teams. Nevertheless, no actuator was able to reproduce the forces and speeds of human muscles. Focusing on humanoid robots, a continuous need for enhancing their performances leads to identifying the desired actuator properties. These properties are: i) high power to mass ratio; ii) high integration within the robot body; iii) safe-interaction of the humanoid with the surrounding environment.

The actuation for humanoid robots can be either electrical or hydraulic actuation. Most robotic applications are electrically driven. Generally, electric motors with high gear ratio drives are popular because of their small size and cheap price. In

addition, electric motors are proven to be easy to use and control. Significant examples of electrically actuated robots are: ASIMO [3], ROBIAN [4], HRP biped series [5], Johnnie and LOLA [6]. However, electric actuation has several drawbacks. Indeed, electric motors normally produce small torques relative to their size and weight, thereby making reduction sub-systems with high ratios essential to convert velocity into torque. These reduction components are limited and cannot increase indefinitely, which resulted in having reduced dynamic capabilities systems [7].

The other actuation solution is based on hydraulic technology. It has several advantages, which mainly include: 1) high power to mass ratio; 2) ability to produce high torque at low speed; 3) the high stiffness compared to electric ones; 4) the ability to perform continuous, intermittent, reversing and stalled motions; 5) the ability to emulate human musculo-skeletal systems by means of high-bandwidth force control. Examples of robots using hydraulic actuation include: Bigdog [8], Sarcos [9] and HyQ [10]. However, this type of actuators has its main

drawbacks. The major one is due to the necessity of a central Hydraulic Power Unit to supply high-pressure fluid to all the robot joints. This unit is always bulky and the leakage from the hydraulic tube connections can cause safety issues, especially in human-robot interaction. Hence, it was necessary to have integrated hydraulic actuators inside the robot and near the joints.

S. Habibi et al. [11] presented a closed loop hydrostatic actuator. This actuator was driven directly from an electric motor without a gear train enabling large speed reductions and corresponding torque amplification. Nevertheless, this actuator had several design constraints to achieve high performance. These constraints include the usage of a symmetrical actuator in addition to appropriate sizing of hydraulic components to minimize the pressure drop. These constraints questioned the supposed compactness of an electrohydraulic actuator dedicated for robotic applications. Recent research was done on the EHA (electro-hydraulic actuator) compactness by Gnesi et al [12] and Takahashi et al [13], in which both presented two EHAs made for aircraft applications. The first presented an EHA with a vane pump and double acting cylinder, while the latter used a similar design but with a piston pump. In 2011, an IEHA (Integrated Electro-Hydraulic Actuator) was developed by Alfayad et al. [14]. Its main objective was eliminating the need for a central pressure source and to be implemented for each joint of the humanoid hydraulic robot HYDROiD. Due to the different pressures needed by the robot joints, each single actuator can be considered autonomous. Thanks to its compactness, the IEHA can be placed as near as possible to the hydraulic actuator (rotary or linear). Hence, the pressure drop is reduced and leakage may only exist inside the actuator. Moreover, the IEHA contains a passive distributor connecting the pump with the actuator. This passive distributor delivers the oil between the pump and the actuator without the need of flipping the direction of the electric motor driving the pump. Hence, the effect of dead band is avoided enhancing the position control of the actuator. In addition to the dead band elimination, the presence of the passive distributor enables the IEHA to handle any asymmetrical actuator.

The main objective for the IEHA is to be implemented on the humanoid robot HYDROiD. Hence, the human robot interaction and compliance are of high priority. There are different ways to ensure that the robot does not risk injuring the user.

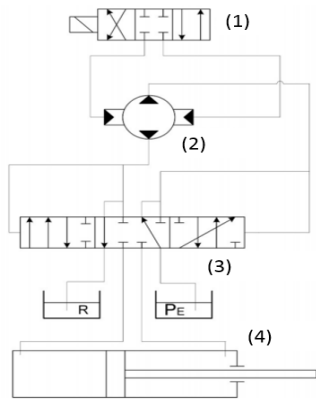
One approach to soft human robot contact is back-drivability. This ability enables the mechanical system to move the input axis from the output axis. In other words, the force applied from output axis of the actuator must be greater than force lost in the actuator due to static friction [15]. A more advanced approach is to apply an active compliance, which can be reached through accurate force/position control [16]. Both of these approaches need a complete dynamic model of the actuation system. In our case another reason is added, which is the unique small dimensions of the IEHA (80mmX40mmX40mm) shown in Fig. (1). This dynamic model will be used in the future to choose the best control strategy to ensure the back-drivability. In addition to studying another uncertainties for the future prototypes. Meanwhile, a sim-mechanics model for the system is introduced to validate the mathematical model and the results of IEHA dynamic simulations are introduced.



FIG. 1: Photo of the IEHA actuator

## 2 Description of the electro-hydraulic actuator (IEHA)

The integrated hydraulic actuator (IEHA) is based on the power transmission from an electric motor to a hydraulic actuator. The basic idea consists of converting the electric power to mechanical one by using a highly integrated micro-pump producing pressure and flow (shown in Fig.2). This energy converter contains an in-built micro-valve that controls the eccentricity. The radial pump is connected to the output piston (linear or rotary) through a passive distributor. In order to simplify the figure, only two of the pump's micro-pistons are shown. Since the passive distributor response is very fast compared to the rest of the components, its dynamics can be neglected in the present study. In this section, the functioning principle of the micro-pump and the micro valve are detailed.



**FIG. 2:** Simplified IEHA diagram with a linear hydraulic cylinder. (1) is the micro-valve, (2) is the micro pump, (3) is the passive distributor and (4) is the output actuator.

### 3 Dynamics of the system

In this section, the necessary hydraulic and mechanical equations of the dynamic model are presented. These equations are based on the prototype of IEHA where the micro radial pump delivers flow from a high-pressure supply to one side of the cylinder at each instant. The other side of the cylinder is connected to an atmospheric reservoir. The way the micro radial pump is connected to the output cylinder (chamber A or B) depends on the sign of the eccentricity and is done by the passive distributor. The dynamics of the passive distributor are not considered, because it has a very fast response time compared to the rest of the system.

#### 3.1 Equations of the micro-pump

To produce hydraulic energy in the authors proposed solution [13], a micro radial pump is used to deliver the hydraulic power required. The flow discharge of such pump can be controlled by modifying the eccentricity of the main shaft driven by the electric motor with respect to the housing. For a given direction of rotation of shaft, fluid enters the pump, and the centrifugal forces and hydraulic pressure push the micro-pistons to the walls of the housing during half of the rotation cycle,  $[0, \pi]$ , where the corresponding micro-pistons are connected to the intake port. As the rotor continues around, the vanes sweep the fluid to the opposite side. For the other half of the cycle  $[\pi, 2\pi]$ , the micro-piston volume decreases and fluid exits the discharge port. Fig.3 presents the hydraulic circuit of the IEHA model. The distance between the bottom of chamber and the centre of the shaft is denoted as  $d$ , while  $R_b$  is the

radius of the carriage.  $h_1$  is the distance between the micro-piston of length  $L_p$  at the dead bottom position and the bottom of its chamber. In the same way,  $h_2$  is the distance between the micro-piston at the high dead point and the bottom of its chamber as given in Equations 1 and 2. The piston stroke is defined by the volume of fluid produced during a rotation for a given eccentricity ( $E$ ). In order to calculate the variation of the micro-pump stroke, the distance that the piston travels during half-rotation corresponding to either the intake or the discharge, is determined.

$$R_b = h_1 + E + L_p + d \tag{1}$$

$$R_b + E = h_2 + L_p + d \tag{2}$$

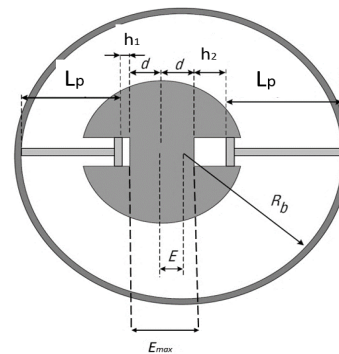


**FIG. 3:** Simplified model of the shaft with two micro-pistons turning inside the housing.

By subtracting equation 1 from 2, the eccentricity can be expressed as:

$$2E = h_2 - h_1 \tag{3}$$

By taking into account the surface of piston  $S_p$ , the volume of oil aspirated and driven back during a rotation is:

$$v_p = 2ES_p \tag{4}$$

Knowing that the total number of pistons and the rotation speed are denoted as  $N_p$  and  $\Omega$  respectively, the micro-pump average flow  $Q_p$  can be calculated using the following relation:

$$Q_p = N_p v_p \Omega = 2 N_p E S_p \Omega \tag{5}$$

The micro-pump flowrate can be related to the output cylinder piston using the following relation:

$$Q_p = S_v \dot{Y} + \eta v_v P'_{v1} \quad (6)$$

Where  $S_v$  is the cross-sectional area of the linear actuator,  $\eta$  is the coefficient of compressibility,  $v_v$  is the volume of the actuator chamber and  $P'_{v1}$  is the pressure in this actuator chamber.

### 3.2 Equations of the micro-valve

The micro-valve main function is to adjust the eccentricity of the carriage. The pistons inside the carriage have two extreme positions, in which the produced flow can be varied between them. However, in order to actuate this valve, a relatively large electric or hydraulic signal is needed. In our case the actuation of the micro-valve is achieved through a voice coil. According to the parameters presented in Appendix I, the required force needed for the micro-valve actuation is calculated as:

$$F_{max} = P n_c \pi \left(\frac{D_p}{2}\right)^2 \quad (7)$$

But in order to stabilize the pump carriage, two simple effect jacks are added on both sides of the pump carriage. These two jacks, denoted as ( $CH_{e1}$  and  $CH_{e2}$ ), are shown in Fig.4.

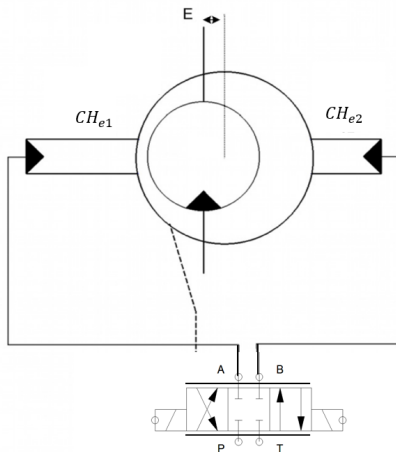


FIG.4 The hydraulic scheme of the micro-valve controlling the eccentricity of the pump carriage.

In order to calculate the resultant flow rate of the micro-valve. The opening of the micro-valve (denoted as  $\Sigma$ ) is expressed as:

$$\Sigma = 2\pi R (X - E) \quad (8)$$

By using Bernoulli 's equation between the output opening of the micro-valve and the fluid entrance at

the carriage, the flow  $Q_e$  created by the micro-valve can be calculated as:

$$Q_e = C_d \Sigma V_D \quad (9)$$

Where  $V_D$  is considered the velocity of the fluid at the fluid entrance of the carriage and can be expressed as:

$$V_D = \sqrt{2 \Delta P / \rho} \quad (10)$$

By substituting eq. (8) and eq. (10) in eq. (9),

$$Q_e = 2\pi R C_d (X - E) \sqrt{2((P_s/2) - \xi)} \quad (11)$$

Where  $P_s$  is the supply pressure and  $\xi$  is the pressure difference resulting from the motion of the micro-valve.

### 3.3 Equations of the linear actuator

By applying Bernoulli 's equations between the pistons located at the side of the micro-pump and the actuator pistons.

$$\frac{v_{p1}^2}{2} + \frac{P_{p1}}{\rho} = \frac{v^2}{2} + \frac{P_v1}{\rho} \quad (12)$$

$$\frac{v_{p2}^2}{2} + \frac{P_{p2}}{\rho} = \frac{v^2}{2} + \frac{P_v2}{\rho} \quad (13)$$

Where  $V_{pi}$  is the oil velocity in chamber  $CH_{pi}$ . Also, in order to calculate these velocities, a simplified structure of the pump barrel is considered (shown in Fig.5), where just two pistons named  $P_1$  and  $P_2$  are presented. The piston named  $P_1$  is the piston during aspiration mode ( $\theta_1 = \omega t$ ). While the second  $P_2$  is the piston during expulsion mode ( $\theta_2 = \omega t + \pi$ ).

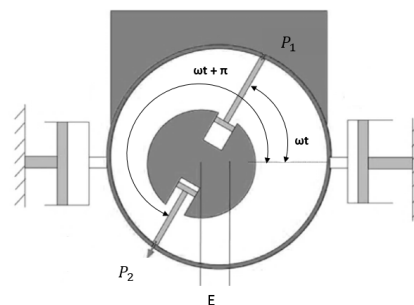


FIG.5 Simplification of pump barrel structure.  $P_1$  and  $P_2$  are the pistons between the sides of the micro-pump and the actuator chambers. E is the eccentricity between the micro-pump and the barrel.

From equations (13) and (14) the side piston velocities can be described as:

$$V_{p1} = +E\omega \sin(\omega t) - \frac{E^2 \omega \sin(\omega t) \cos(\omega t)}{\sqrt{R_b^2 - E^2 \sin(\omega t)^2}} \quad (14)$$

$$V_{p2} = -E\omega \sin(\omega t) - \frac{E^2 \omega \sin(\omega t) \cos(\omega t)}{\sqrt{R_b^2 - E^2 \sin(\omega t)^2}} \quad (15)$$

Additionally, by subtracting equations (12) and (13) it leads to:

$$\Delta P_v = \Delta P_p + \frac{\rho}{2} (V_{p2}^2 - V_{p1}^2) \quad (15)$$

Since the term can be considered negligible due to geometrical constraints and  $V_{p2} \approx -V_{p1}$ , therefore:

$$\Delta P_v = \Delta P_p \quad (16)$$

Where  $P_p$  is pressure of the actuating piston. By applying newton's law on the load, the final relation for the output actuator is:

$$m\dot{Y} = S_v \Delta P_v - F_c \quad (17)$$

$F_c$  is the external force applied on the output actuator,  $m$  is the external mass,  $\dot{Y}$  and  $S_v$  are the acceleration and the active area of the output actuator respectively.

### 4 Virtual Model

Compactness of our electro-hydraulic actuator makes it difficult to measure the internal variables of the system, such as the micro pump eccentricity and internal pressure drop. Moreover, it is important to study the effect of configuring the internal variables (e.g. the dimensions of different mechanical parts) on the behavior of the system before modifying the system design in future prototypes. Therefore, development of a virtual model of the IEHA provides deeper understanding of the system and can be considered as an efficient platform for further system optimization. The effectiveness of the developed virtual model allows a quick and accurate evaluation of the internal parameters early in the design and development stage.

For this purpose, MATLAB-Simulink was used to model all the dynamic equations of the IEHA actuator, as well as fluid properties such as bulk modulus and internal leakage. The micro-valve takes signal  $X$  as an input, the resulting eccentricity  $E$  is applied to the micro-pump which is simulated as 10 individual micro-pistons. The flow produced by the

micro-pistons is sent to the passive distributor which directs it to side A or B of the linear actuator. The electric motor has been modeled as constant input rotating at a fixed speed. The used parameters values are given in Appendix I.

The following simulation results show the variation of internal parameters against a step input of 0.025 [cm] of the micro valve position  $X$ . Generally, the input command  $X$  decides how much the micro-valve should be opened and as the pressure in the chamber increases, the carriage moves and  $E$  changes. Fig.6 shows the response of the carriage eccentricity,  $E$ , while it follows the micro-valve displacement  $X$ . As seen in the forementioned figure, the time response of  $E$  is around 0.008[s] and it follows the input  $X$  with a negligible delay.

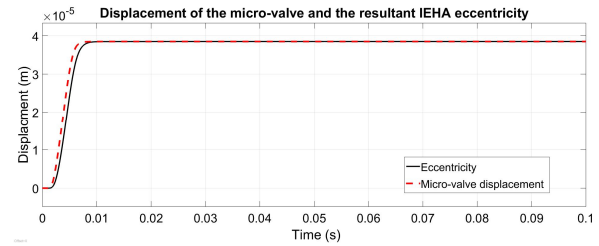


FIG.6 Input  $X$  to the micro-valve and the carriage eccentricity  $E$  following  $X$ . The response time of  $E$  is 0.008[s]

In order to illustrate the pressure variation in the micro-pistons, the variations of the output cylinder pressures are linked to the oscillation of flow. By looking at pump flow curve (Fig.7), it is clear that the flow rises up to 1.4 m<sup>3</sup>/s in the first 0.005 s, then oscillates around the 1 m<sup>3</sup>/s. This oscillation is due to the fluid rippling from the micro-radial pump. There is also a slight peak in the beginning, the faster the eccentricity the bigger this peak of flow is.

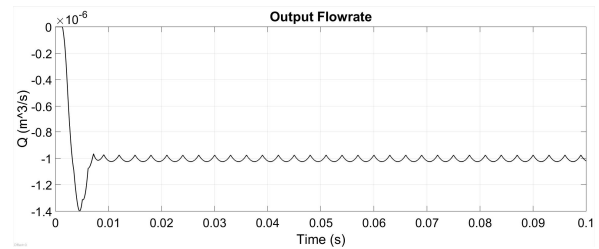
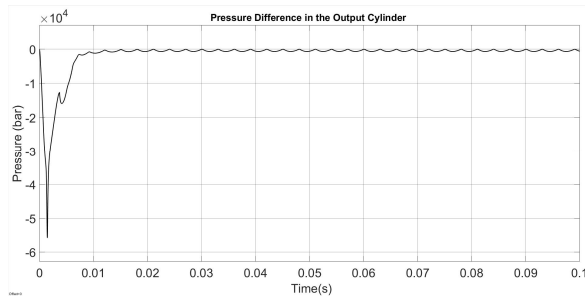
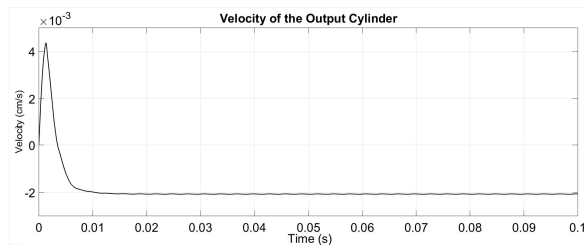


FIG.7 Flow produced by the micro-radial pump



**FIG.8** Pressure difference in the chambers of the output cylinder,  $P_{Cyl B} - P_{Cyl A}$

In the beginning of the cylinder’s movement as shown in Fig.8, the pressure across the cylinder increases due to fluid compressibility. And as the load starts to move, the pressure difference across the cylinder drops and the velocity reaches the stable value of 2.0 [cm/s] as shown Fig.9. The pressure difference across the output rises to (5.5 bar), then gradually decreases till zero. This will lead also to a gradual change in the output piston position Y as shown in Fig.10. This is continued till the occurrence of a change in input of the micro-valve signal.



**FIG. 9** Velocity of the output piston  $\dot{Y}$

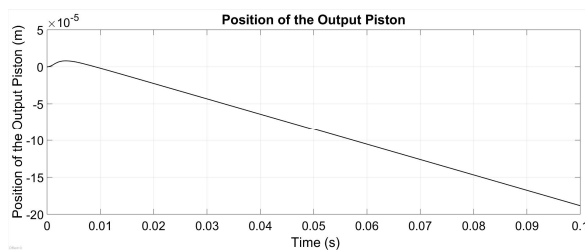


**FIG. 10** Position of the output piston Y

In these results, the output flow of the pump seems to immediately increase the pressure force in the output cylinder and make the piston velocity increase to a stable value. This is because the dynamics of the passive distributor are not taken into account in this model in Simulink.

## 5 Validation of the Simulink model

The CAD model of the IEHA actuator was imported in Sim-mechanics tool-box in MATLAB. In this toolbox, the imported CAD file in this case is usually considered an accurate representation for the system. The imported sim-mechanics model in this case has the same characteristics of the original CAD Model [18]. These characteristics include the system geometry, inerial properties ...etc. The IEHA sim-mechanics model is shown in Fig.10.

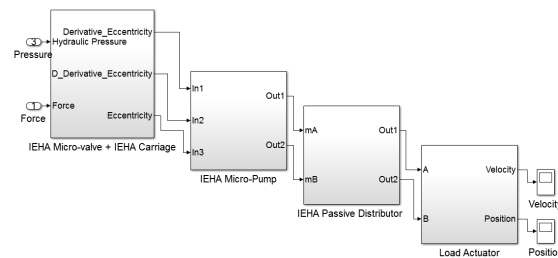


**FIG.11** The sim-mechanics Model of the IEHA actuator  
The system is simulated using the same input parameters used for the virtual model in section 5 but with the sim-mechanics model this time. Simulation results include the displacement of the micro-valve, flow produced by the micro-pump, pressure difference in the actuator chambers, velocity of the output piston and position of the output piston. Those results are shown in Fig. (12 to 16) respectively.

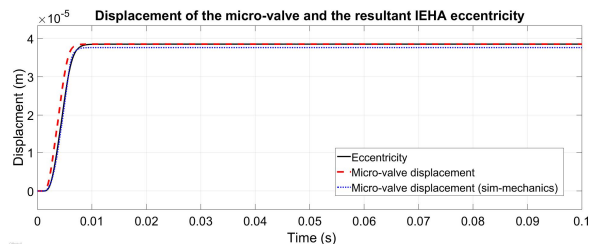


**FIG.12** Displacement of micro-valve in Simulink and sim-mechanics models in response to the change in eccentricity

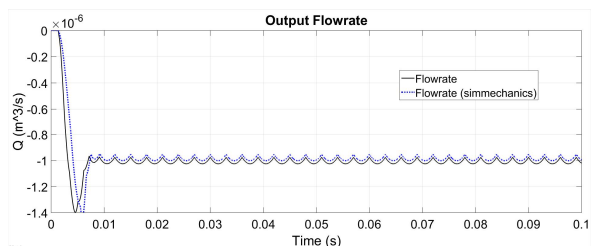


**FIG.13** Flow produced by the micro-radial pump



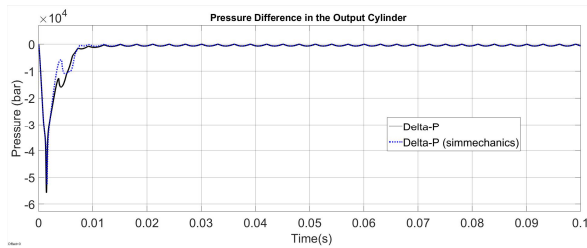


**FIG.14** Pressure difference in the chambers of the output cylinder,  $P_{cyl A} - P_{cyl B}$

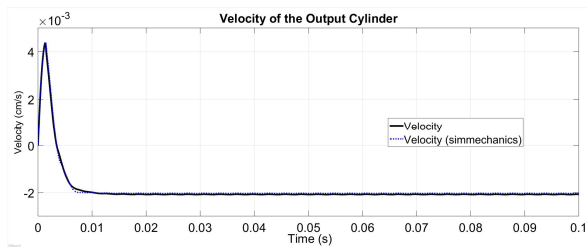


**FIG. 15** Velocity of the output piston  $\dot{Y}$

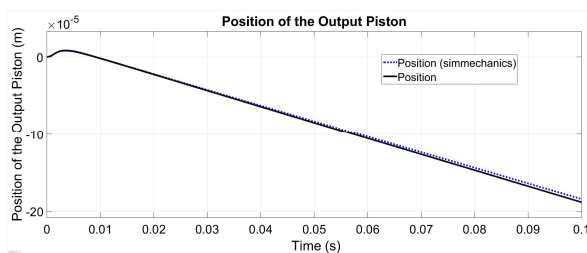


**FIG. 16** Position of the output piston  $Y$

These results show a slight difference between the mathematical model derived in section 5 and the simmechanics model presented in this section. As the system experience slightly lower flow, lower difference in pressure, lower and position for the output actuator than the results from the Simulink model.

Each of previous models have their advantages and disadvantages. Using Simulink to model the system helped us to have a better understanding of the mathematical equations underlying the system. The simulation is also faster compared to the Simmechanics model, but very sensitive to the simulation step time. The Simulink model run with a fixed step time, so it can be compiled into C language and inserted easily in an external program. However, using Simulink on a complex system like ours has its own limits. For examples hard stops, (e.x. a piston at the end of its stroke), are modeled as saturation, and if we want to model the impact forces in these cases, we should add spring equations manually; this would increase the order of the system and the Simulink

solver would be more sensitive to time step; however, decreasing the step time can make the simulation too slow.

## Acknowledgement

This work was mainly funded by BIA- TURNKEY TEST SYSTEMS company.

## 6 Conclusion

In this paper, a detailed mathematical model is presented for electro-hydraulic actuator (IEHA). Due to the small size of the IEHA actuator, the verification of such dynamic model is needed. Because an accurate dynamic model is a vital tool for cost reduction and speeds up the design process in future prototypes. To verify the mathematical model at hand, a sim-mechanics model for the IEHA is introduced and compared with the original model. The results showed that we can depend on the derived mathematical model to represent the IEHA actuator and modify it in future prototypes.

For future work, the internal parameters of the hydraulic mathematical model such as leakage and compressibility are not constant and vary with time and temperature. Hence, a further work must consider a better solution to identify the internal states of the system. On the other hand, the passive distributor model has to be included in order to get a complete description of the IEHA model. The new virtual model presented can be used for manufacturing other actuator prototypes with all of its inner parameters identified. Finally, the usage of the IEHA to actuate active hydraulic joints for the hydraulic humanoid robot HYDROiD is considered.

## References:

- [1] S. Alfayad, F. Ouezdou, F. Namoun, Converter for converting mechanical energy into hydraulic energy and robot implementing said converter, *US Patent App.* 12/934,592 (Apr. 14 2011).
- [2] C. Semini, N. G. Tsagarakis, E. Guglielmino, M. Focchi, F. Cannella, and D. G. Caldwell, "Design of HyQ - a hydraulically and electrically actuated quadruped robot," *Proc. Inst. Mech. Eng. Part I J. Syst. Control Eng.*, vol. 225, no. February, pp. 831–849, 2011.

- [3] Sakagami, Y., Watanabe, R., Aoyama, C., Matsunaga, S., Higaki, N. and Fujimura, K. "The intelligent ASIMO: system overview and integration". In *Proc. of IROS*, 2002, 2478- 2483.
- [4] A. Konno, R. Sellaouti, F. B. Ouezdou, "Design and Development of the Biped prototype ROBIAN", *ICRA 2002*. P. 1384 - 1389.
- [5] K. Kaneko, F. Kanehiro, M. Morisawa, K. Akachi, G. Miyamori, A. Hayashi, and N. Kanehira, "Humanoid robot HRP-4 - Humanoid robotics platform with lightweight and slim body," *IEEE International Conference for Intelligent Robotic Systems*, pp. 4400-4407, 2011.
- [6] T. Buschmann, S. Lohmeier, and H. Ulbrich, "Humanoid robot Lola: Design and walking control," *J. Physiol. Paris*, vol. 103, no. 3-5, pp. 141-148, 2009.
- [7] X. Zhou and S. Bi, "A survey of bio-inspired compliant legged robot designs," *Bioinspiration & biomimetics*, vol. 7, no. 4, p. 041001, 2012.
- [8] M. Raibert, K. Blankespoor, G. Nelson, and R. Playter, "Bigdog, the Rough-Terrain Quadruped Robot," in *Proceedings of the 17th World Congress*, 2008, pp. 10823-10825.
- [9] D. C. Bentevegna, C. G. Atkeson, and J. Y. Kim, "Compliant control of a hydraulic humanoid joint," *Proc. 2007 7th IEEE-RAS Int. Conf. Humanoid Robot. HUMANOIDS 2007*, pp. 483-489, 2008.
- [10] C. Semini, "HyQ - Design and Development of a Hydraulically Actuated Quadruped Robot," *Darwin*, no. April, p. 210, 2010.
- [11] Saeid Habibi, and Andrew Goldenberg, "Design of a New High Performance Electrohydraulic, Actuator," *Proc. 1999 IEEE/ASME*, vol. 5, no. Figure 2, pp. 158-164, 1999.
- [12] E. Gnesi, J-C. Maré, J. L. Bordet "Modeling of EHA Module Equipped with Fixed-Displacement Vane Pump," *13th Scand. Int. Conf. Fluid Power, SICFP2013*, pp. 141 - 153, 2013.
- [13] N. Takahashi, T. Kondo, and M. Takada, "Development of prototype electro-hydrostatic actuator for landing gear extension and retraction system" *Sumitomo Precision Products Co., Ltd.*, no. c, pp. 165-168, 2008.
- [14] S. Alfayad, F. B. Ouezdou, F. Namoun, G. Cheng, "Lightweight High Performance Integrated Actuator for Humanoid Robotic Applications: Modeling, Design & Realization" in *Proc. IEEE Int. Conf. on Robotics and Automation (ICRA)*, Kobe, Japan, 2009.
- [15] H. Kaminaga, T. Yamamoto, J. Ono, Y. Nakamura, "Backdrivable miniature hydrostatic transmission for actuation of anthropomorphic robot hands", 2007, *7th IEEE-RAS International Conference on Humanoid Robots*, Nov.29.2007-Dec.1.2007, pp.36-41.
- [16] Q. Zhu, Y. Mao, R. Xiong, and J. Wu, "Adaptive Torque and Position Control for a Legged Robot Based on a Series Elastic Actuator," *Int. Journal of Advanced Robotics Systems*, p. 1, 2016.
- [17] S. Alfayad, F. B. Ouezdou, F. Namoun, and G. Gheng, "High performance integrated electro-hydraulic actuator for robotics - Part I: Principle, prototype design and first experiments," *Sensors & Actuators, A Phys.*, vol. 169, pp. 115-123, 2011.
- [18] J. Zatopek, "Various Support Software Tools Using In Simulation and Identification of a Non-linear Unstable System of Motion," *WSEAS TRANSACTIONS on SYSTEMS*, vol. 15, pp. 321-328, 2016.



## Appendix I

Parameter	Physical Quantity	Value
$P_s$	Supply pressure of micro-valve	5 bar
$r_{tig}$	Micro-valve radius	0.25 cm
$S_e$	Carriage active surface area	1.644 cm <sup>2</sup>
$m_e$	Carriage mass	0.091 kg
$E_{max}$	Maximum eccentricity	0.025 cm
$v_e$	Chamber volume of carriage	0.0822 cm <sup>3</sup>
$\beta$	Bulk modulus	800 MPa
$C_d$	Vena contracta coefficient	0.62
$\rho$	Fluid density	840 kg/m <sup>3</sup>
$P_{rp}$	Supply pressure of micro-pump	10 bar
$\omega$	Electric motor rotational speed	2000 rpm
$N$	Number of micro-pistons	10
$r_{rp}$	Micro-pump in-out radius	0.2 cm
$m_p$	Micro-piston mass	0.5 g
$S_p$	Micro-piston surface area	0.197 cm <sup>2</sup>
$L_p$	Micro-piston stroke	0.3 cm
$R_b$	Interior ring radius	0.3 cm
$d$	Distance between chamber bottom & shaft center	0.4 cm
$m$	Load mass	8 kg
$v_c$	Chamber volume of output cylinder	23.562 cm <sup>3</sup>
$S_c$	Output cylinder surface area	2.356 cm <sup>2</sup>